Supporting Information

Amprazi et al. 10.1073/pnas.1322065111

SI Materials and Methods

Small Angle X-ray Scattering Analysis. At the SWING beamline of the SOLEIL synchrotron, small angle X-ray scattering (SAXS) data were collected from the elution peaks of a size exclusion chromatography column as follows: Protein samples (900 μg of protein in 40 μL of storage buffer) were loaded at 25 °C onto a pre-equilibrated Shodex KW402.5–4F 150-kDa column and passed with a flow rate of 150 μL/min through the X-ray beam; 250 frames were collected over a volume that included the elution peak. Approximately 20 frames were collected before the protein reached the beam for background subtraction purposes. Scattering was recorded with an AVIEX170 × 170 CCD detector over a momentum transfer range of $q = 0.01–0.5$ Å^{-1} [$q = 4\pi\sin(\theta)/\lambda$, with 2θ being the scattering angle and $\lambda = 1.03$ Å the wavelength of X-rays].

The radius of gyration (R_g) was calculated from the slope of the Guinier plot using the software PRIMUS (1). The forward scattering intensity $I(0)$ was estimated through extrapolation of the Guinier plot at a scattering angle of $2\theta = 0^o$ and used to calculate the molecular mass. The evolution of $I(0)$ in relation to the UV-absorption profile of the sample was used to judge the monospersity of the protein samples (2). Frames corresponding to constant R_g values were used in the SAXS data analysis as they correspond to monodisperse samples.

The dimensionless Kratky plots (3) used in the assessment of the folding states of the proteins studied have a theoretical maximum value close to 1.1 for $qR_g = \sqrt{3}$ for a fully folded, single-domain globular protein. In contrast, for a completely random chain, the curve rises with increasing angle to a plateau at a value between 1.5 and 2 and at high q increases further, depending on the rigidity of the chain.

Circular Dichroism Measurements. For collection of circular dichroism (CD) spectra with a J-810 CD spectropolarimeter, a quartz cuvette of 1-mm path length was used and protein concentrations of 0.15 mg/mL in 20 mM Tris·HCl buffer, pH 8.0, with 5 mM NaCl. Far-UV spectra (260–195 nm) were measured with 50 nm/min scanning speed, a 2-min response time, and three accumulations. The Spectra Manager program (Jasco) was used for buffer subtraction and unit conversions to mean residual ellipticities.

The singular value decomposition (SVD) analysis (4) of the far-UV CD spectra was performed to determine significant independent states in the unfolding transition. As reported for other proteins (5), the unfolding process can be modeled using the significant species determined by SVD on the base of the characteristics of the SVD basis vectors (U) and the temperature dependence of their associated coefficients (V).

1. Konarev PV, Volkov VV, Sokolova AV, Koch MHJ, Svergun DI (2003) PRIMUS: A Windows PC-based system for small-angle scattering data analysis. *J Appl Cryst* 36(5):1277–1282.
2. David G, Perez J (2009) Combined sampler robot and high-performance liquid chromatography: A fully automated system for biological small-angle X-ray scattering experiments at the Synchrotron SOLEIL SWING beamline. *J Appl Cryst* 42(5):892–900.
3. Durand D, et al. (2010) NADPH oxidase activator p67(phox) behaves in solution as a multidomain protein with semi-flexible linkers. *J Struct Biol* 169(1):45–53.
4. Manavalan P, Johnson WC, Jr (1987) Variable selection method improves the prediction of protein secondary structure from circular dichroism spectra. *Anal Biochem* 167(1): 76–85.
5. Gazi AD, et al. (2008) Evidence for a coiled-coil interaction mode of disordered proteins from bacterial type III secretion systems. *J Biol Chem* 283(49):34062–34068.

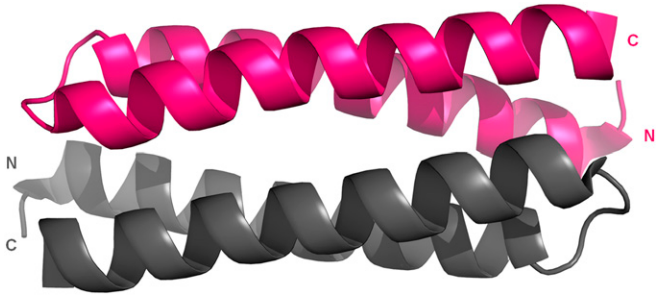

Fig. S1. Schematic representation of PG. The PG dimer is shown; the two monomers are colored individually. The N and C termini of the protein are labeled. The figure was generated using the 2010 PyMOL Molecular Graphics System, Version 1.3r1 (1).

1. Schrodinger LLC (2010) The PyMOL Molecular Graphics System, Version 1.3r1.

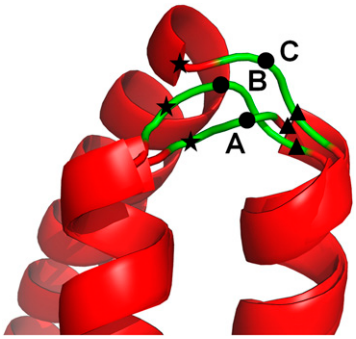

Fig. S2. Loop structures for Rop and its mutants. Three different loop conformations are shown: (*A*) WT (1ROP), (*B*) PG (4DO2, chainA), and (*C*) A31P (1GMG). The triangle indicates the Cα position of residue in position 29; the circle, position 30; and the star, the critical loop position 31. The figure was generated using the 2010 PyMOL Molecular Graphics System, Version 1.3r1 (1).

1. Schrodinger LLC (2010) The PyMOL Molecular Graphics System, Version 1.3r1.

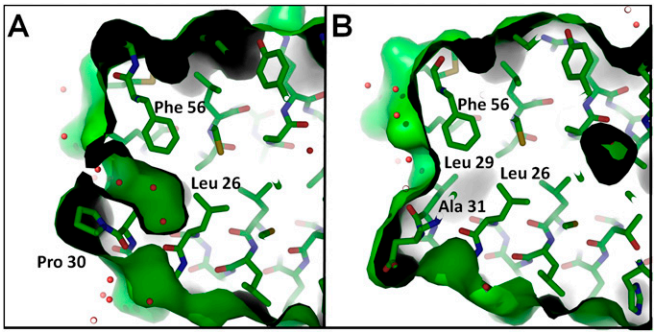

Fig. S3. Solvent-accessible surfaces for the region near the end of the PG and WT helical bundles that comprise the loop of one subunit of the dimer and the N and C termini of the other subunit. (*A*) The PG dimer and the hydrated pocket created by the mutation. Water molecules are shown as small spheres. (*B*) The WT dimer. In both cases, hydrophobic residues close to the end of the protein core are labeled. Due to the proximity to disordered C-terminal residues, the water molecules have been added conservatively for both structures. The figure was generated by the PyMOL Molecular Graphics System, Version 1.3r1 (1).

1. Schrodinger LLC (2010) The PyMOL Molecular Graphics System, Version 1.3r1.

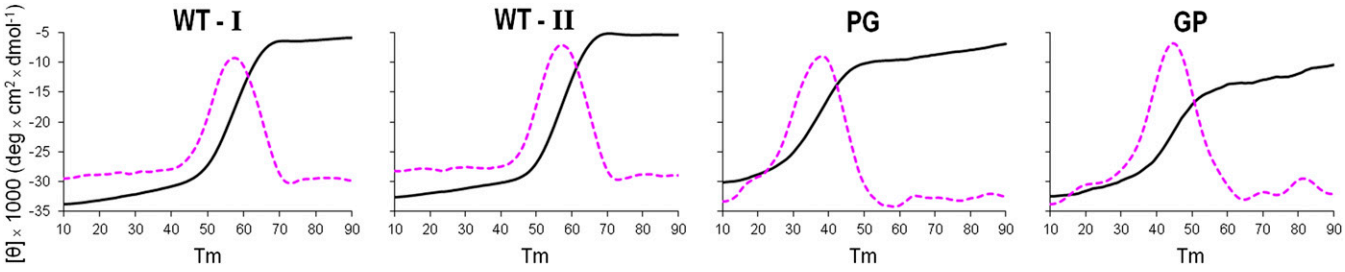

Fig. S4. Thermal unfolding curves for WT, PG, and GP in the absence of reducing agent. Melting curves (black line) monitoring the variation of the CD signal at 222 nm with the temperature. The melting temperature (T_m) of each protein is determined by the maximum of the first derivative (purple dashes) of the melting curve. The T_m values for WT-I and II are 58 °C; for PG, 39 °C; and for GP, 44 °C. In all cases, the CD signal has been transformed into mean residue ellipticity.

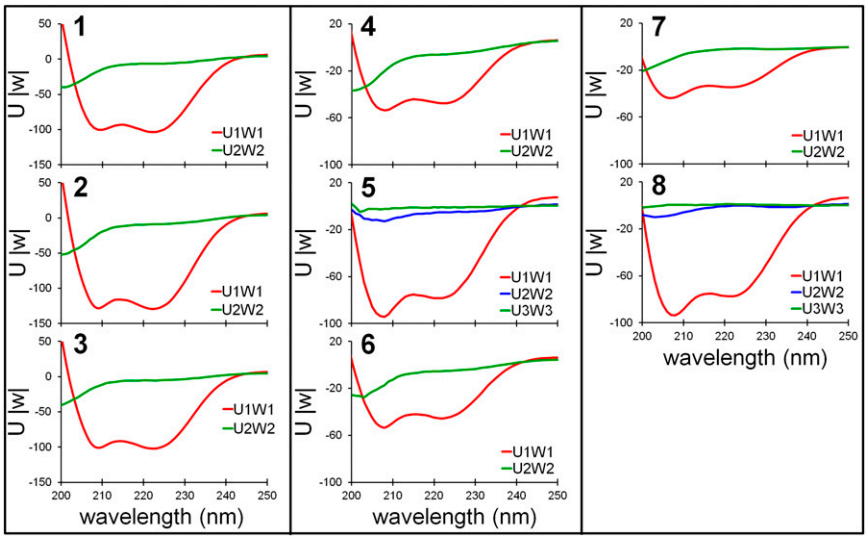

Fig. S5. SVD analysis of the far-UV CD spectra recorded at different temperatures. The first two (or three) basis vectors u_i, weighted by the singular values w_i, are shown in different colors. The states shown suffice to model the CD spectra recorded, as all other states are negligible. The analysis has been performed on the following sets of CD spectra (Fig. 4): 1, WT in the presence of β-met; 2, WT, no β-met, peak I (Fig. 2*B*); 3, WT, no β-met, peak II (Fig. 2*B*); 4, A31P in the presence of β-met; 5, A31P, no β-met, peak I (Fig. 2*B*); 6, A31P, no β-met, peak II (Fig. 2*B*); 7, PP in the presence of β-met; and 8, PP, no β-met.

Table S1. Crystallographic refinement and structure validation statistics for PG

Data collection and refinement	
Resolution, Å	18.5–1.4 (1.46–1.4)
Reflections	21,133
R factor*/R_{free}†, %	15.9 (19.9)*/18.7 (30.0)*
Average B-factors, Å^2	
Wilson B-factor	20.6
All atoms	17.6
Main-chain atoms	12.4
Side-chain atoms	21.4
Waters	32.8
No. of protein atoms	935
No. of water molecules	169
No. of residues	114
Structure validation	
rmsd	
Bond lengths, A°	0.027
Bond angles, °	2.405
Residues in the Ramachandran plot	
Most favored regions	112 (98.2%)
Additionally allowed regions	2 (1.8%)

Values in parentheses refer to the outer resolution shell (1.46–1.40 Å).
*R factor $= \Sigma|F_{obs} - F_{calc}|/\Sigma|F_{obs}|$.
†R_{free}, an R factor for a selected subset (10%) of the reflections that was not included in prior refinement calculations.

Table S2. Comparison of the crystal structure of PG with the structures of WT and A31P

		WT	A31P		
	PDB code	1ROP	1GMG A	1GMG B	1B6Q
I: subunits					
PG	4DO2 A	0.54	6.33	5.66	5.13
	4DO2 B	0.59	6.34	5.75	5.09
II: dimers					
PG	4DO2	0.59	8.921	8.81	8.38
PG	4DO2	0.59	8.92	8.8	8.38

(I) rmsd for structure comparisons at the level of individual subunits (A and B). In the case of WT and one form of A31P (PDB ID code 1B6Q), only one polypeptide chain is used in the comparisons as both subunits of the proteins are structurally identical, being related by a crystallographic dyad. (II) rmsd for comparisons at the level of dimers. PDB, Protein Data Bank.

Table S3. φ and ψ conformational angles for the loop regions of WT and selected variants

	Position 29			Position 30			Position 31		
Protein	Residue	φ	ψ	Residue	φ	ψ	Residue	φ	ψ
WT	Leu	−90	−1	Asp	57	38	Ala	−94	89
A31P (1B6Q)	Leu	−107	168	Asp	−74	157	Pro	−47	−53
A31P (1GMG)	Leu	−90	155	Asp	−73	161	Pro	−43	−42
PG	Leu	−114	159	Pro	−77	−5	Gly	−83	90

The loop conformations of PG (PDB ID code: 4DO2, chain A), WT (1ROP), and A31P (orthorhombic form: PDB ID code 1B6Q, chain A; monoclinic form: PDB ID code 1GMG, chain A) are given.